Photophysics of Aromatic Molecules with Low-Lying $\pi\sigma^*$ States: Excitation-Energy Dependence of Fluorescence in Jet-Cooled Aromatic Nitriles

Ricardo Campos Ramos,[†] Takashige Fujiwara,[†] Marek Z. Zgierski,[‡] and Edward C. Lim*,[†]

Department of Chemistry and The Center for Laser and Optical Spectroscopy, The University of Akron, Akron, Ohio 44325-3601 and Steacie Institute for Molecular Sciences, National Research Council of Canada, Ottawa, Ontario, Canada

Received: February 21, 2005; In Final Form: May 19, 2005

Excitation-energy dependence of fluorescence intensity and fluorescence lifetime has been measured for 4-dimethylaminobenzonitrile (DMABN), 4-aminobenzonitrile (ABN), 4-diisopropylaminobenzonitrile (DIABN), and 1-naphthonitrile (NN) in a supersonic free jet. In all cases, the fluorescence yield decreases rather dramatically, whereas the fluorescence lifetime decreases only moderately for S_1 ($\pi\pi^*$, L_b) excess vibrational energy exceeding about 1000 cm^{-1}. This is confirmed by comparison of the normalized fluorescence excitation spectrum with the absorption spectrum of the compound in the vapor phase. The result indicates that the strong decrease in the relative fluorescence yield at higher energies is due mostly to a decrease in the radiative decay rate of the emitting state. Comparison of the experimental results with the TDDFT potential energy curves for excited states strongly suggests that the decrease in the radiative decay rate of the aminobenzonitriles at higher energies is due to the crossing of the $\pi\pi^*$ singlet state by the lower-lying $\pi\sigma^*_{C\equiv N}$ singlet state of very small radiative decay rate. The threshold energy for the fluorescence "break-off" is in good agreement with the computed energy barrier for the $\pi\pi^*/\pi\sigma^*$ crossing. For NN, on the other hand, the observed decrease is in fluorescence yield at higher excitation energies can best be attributed to the crossing of the $\pi\pi^*$ singlet state by the $\pi\sigma^*$ triplet state.

Introduction

State switch from a bright (fluorescent) electronically excited state to a dark electronic state leads to an abrupt break-off of fluorescence (at higher excess vibrational energies) in gas phase under collision-free conditions, and a strong thermal quenching of fluorescence in solution. One of the most interesting examples of such a state switch is the $\pi\pi^* \rightarrow \pi\sigma^*_{C\equiv C}$ crossing in diphenylacetylene (DPA) and its derivatives.[1,2] DPA exhibits the fluorescence break-off,[3] characteristic of the state switch[1] and a strong picosecond (ps) transient absorption in the visible (red) region that can be assigned[1,2] to the $\pi\sigma^*$ state. An analogous state crossing is also expected for aromatic nitriles possessing low-lying $\pi\sigma^*_{C\equiv N}$ state. Time-dependent DFT (TD-DFT) calculations on 4-dimethylaminobenzonitrile (DMABN)[6] and 4-aminobenzonitrile (ABN),[6] carried out using BP86/6-311++G** level of theory, indeed show low-energy (~0.14 eV) crossing between the initially excited $\pi\pi^*$ state and a lower-lying $\pi\sigma^*_{C\equiv N}$ state. The calculation also predicts the occurrence of a highly allowed $\pi\sigma^* \leftarrow \pi\sigma^*$ transition in the visible region. Consistent with these predictions, DMABN and ABN exhibit in solution a strong picosecond transient absorption in the region of 600−800 nm,[4,5,7,8] which can be assigned to the predicted $\pi\sigma^* \leftarrow \pi\sigma^*$ absorption. For jet-cooled 4-diisopropylaminobenzonitrile (DIABN), the fluorescence break-off very similar to that in DPA has been observed for S_1 vibrational energy exceeding about 800 cm^{-1}.[9]

It is significant that the $\pi\sigma^*$ state, formed from the $\pi\pi^* \rightarrow \pi\sigma^*$ state switch is a charge-transfer state in which an electron localized on the phenyl π orbital is promoted to the σ^* orbital localized on the acetylenic unit (i.e., C≡C bond)[1,2] or the cyano (C≡N) group.[6,10] As such, the $\pi\sigma^*$ state could play an important role in the photoinduced charge separation of the electron donor−acceptor (EDA) molecules containing the DPA[2] and benzonitrile[6] motifs. Consistent with this conjecture, the analyses of the picosecond transient absorption spectra of *p*-(dimethylamino)-*p*′-cyano DPA (DACN-DPA) and DMABN strongly suggest that the fully charge-separated intramolecular charge-transfer (ICT) state is formed from the initially excited $\pi\pi^*$ state via the $\pi\sigma^*_{C\equiv C}$ (or the $\pi\sigma^*_{C\equiv N}$) state, following the consecutive reaction scheme: $\pi\pi^* \rightarrow \pi\sigma^* \rightarrow$ ICT.[2,6] The $\pi\pi^* \rightarrow \pi\sigma^*$ state switch is, therefore, of considerable importance to the photophysics and photochemistry of aromatic nitriles in general.

In this paper, we present the excess vibrational energy dependence of fluorescence for jet-cooled DMABN, ABN, DIABN, and 1-naphthonitrile (NN). Comparison of the experimental results with the computed potential energy profiles strongly suggests the occurrence of the low-energy $\pi\pi^*/\pi\sigma^*$ crossing in the four aromatic nitriles.

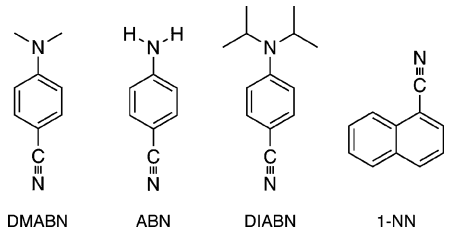

* Corresponding author. Holder of Goodyear Chair in Chemistry. E-mail: elim@uakron.edu. Fax: +330-972-5297.
[†] The University of Akron.
[‡] Steacie Institute of Molecular Science.

10.1021/jp050889b CCC: $30.25
Published on Web 07/22/2005

Methodology

Excitation-energy dependence of laser-induced fluorescence was investigated in a conventional supersonic jet apparatus. The sample of aromatic nitriles (all from Aldrich), used without further purification, was heated to various temperatures (85 °C for DMABN, 70°C for ABN, 100°C for DIABN, and 95 °C for NN) and co-expanded with 2−3 atm helium through a 0.8-mm diameter of a pulsed valve (General Valve) synchronized by a pulse generator (Stanford, DG535) with a duration of ∼400 μs. The laser beam was provided by a dye laser (Lambda Physik, ScanMate) pumped by a Nd:YAG laser (Quanta-Ray GCR-150-10) operated at 10 Hz. The fundamental output was used for generation of the ultraviolet (UV) radiation by frequency doubling with a BBO crystal. Fluorescence, measured perpendicular to both the laser and the supersonic beam by a two-lens system, was collected through a cutoff filter (Schott, UV-34) and detected with a photomultiplier tube (PMT; Hamamatsu R955) at a distance of ∼10 mm from the nozzle. The signal from the PMT was preamplified and fed into a boxcar averager (Stanford, SR250) and interfaced to a personal computer. For normalizing the fluorescence excitation spectra of ABN, DMABN, DIABN, and CNN, laser tuning curves of the Rhodamine 101, Rhodamine B, and Rhodamine 6G dyes were recorded by detecting the laser-scattered light generated in the source chamber through the PMT. Baseline corrections were made to raw data and laser dyes profiles, and the normalization of the excitation spectra were carried out by dividing the raw data intensity by the laser-tuning curve.

The vapor-phase absorption spectra were measured by a Shimazu spectrometer, and the fluorescence excitation spectra were recorded by a Jobin Yvon-SPEX Fluorolog-3 fluorometer.

The fluorescence lifetime measurements were performed by a time-correlated single-photon counting (TCSPC) system implemented by a picosecond laser system. The pulse-train from a dye laser (Coherent, 702-1D), synchronously pumped by a frequency doubling of a mode-locked 76 MHz Nd:YLF laser (Quantronix, 4217ML), was reduced down to typically <15 MHz by a cavity dumper. The laser pulse of ∼5 ps width was then focused into a BBO crystal to generate second-harmonic radiation. The UV light crossed the jet at a distance of 3−5 mm downstream from a CW nozzle, which has an orifice of 100 μm operating at a stagnation pressure of ∼5 atm. Such a high gas flow from the CW nozzle was pumped with a 10 in. diffusion pump (Varian VHS-10; 6600 *l*/s) backed by a rotary pump (Edwards E2M80) through a mechanical booster pump (Edwards EH500A). The fluorescence was collected by using a two-lens system passed through a sharp cutoff filter (>340 nm) and detected with a microchannel plate photomultiplier (MCP; Hamamatsu, R3809U-51). The output of the MCP was fed to an onboard TCSPC module (Becker & Hickl, SPC-300) as a start pulse. Stop pulses were provided from a photodiode (EOT, ET2000), which monitored fundamental laser radiation. The temporal response of the detection system was achieved in less than 45 ps (fwhm). The fluorescence lifetimes were derived by deconvolution procedures, with the instrumental response using nonlinear least-squares fittings.

The time-dependent DFT (TDDFT) energy calculations for the excited singlet states were conducted at the TD/BP86/6-311++G** level of theory using the Gaussian 03 suite of programs at the Ohio Supercomputer Center. The CIS energy of the $\pi\sigma^*$ triplet state of NN was calculated using 6-311++G** basis set.

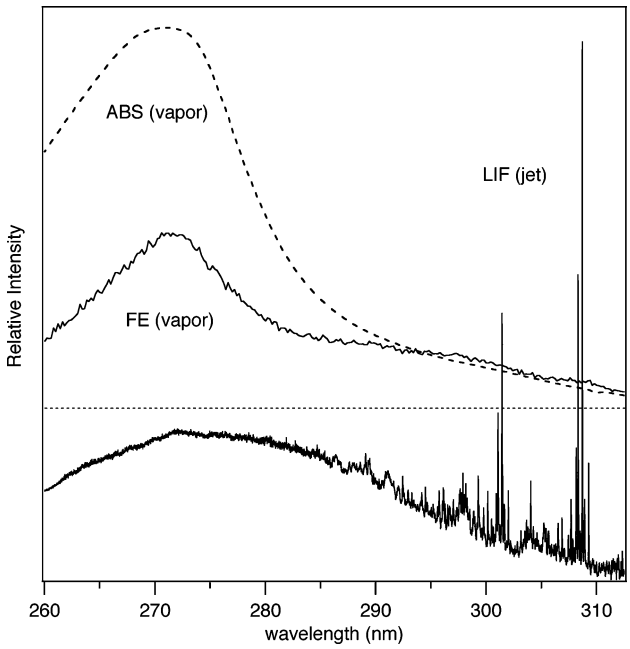

Figure 1. Comparison of laser-induced fluorescence excitation spectrum of DMABN in a free jet and fluorescence excitation and absorption spectrum of a vapor-phase DMABN at about 50 °C, recorded under a collision-free condition. The broad, structureless feature at shorter wavelength in the three spectra represents the $\pi\pi^*$ (L_a) ← S_0 absorption.

Results and Discussion

***p*-Dimethylaminobenzonitrile (DMABN).** In nonpolar solvents and as vapor, the aminobenzonitriles exhibit a small quantum yield of fluorescence, $\Phi_F = k_r/(k_r + k_{nr})$, and a large quantum yield of $S_1 \rightarrow T$ intersystem crossing (ISC). The quantum yield of fluorescence from the $^1\pi\pi^*$ (L_b) state was reported to be 0.18 for DMABN and less than 3×10^{-4} for DIABN in hexane.[11] The highly efficient $S_1 \rightarrow T$ ISC can be traced to the large $^1\pi\pi^*-^3\pi\sigma^*$ and $^1\pi\sigma-^3\pi\pi^*$ spin−orbit coupling.[12] Because of the large nonradiative decay rates (k_{nr}) of the compounds relative to their radiative decay rate (k_r), the measured fluorescence lifetime, $\tau_F = 1/(k_r + k_{nr}) \simeq 1/k_{nr}$, is expected to be very sensitive to the variation in k_{nr}.

Figure 1 presents the normalized fluorescence excitation spectrum of jet-cooled DMABN for the wavelength range of 260−312 nm, which covers the spectral regions of electronic transitions to the two lowest $\pi\pi^*$ states (L_b and L_a in Platt's notation)[13] of the molecule. The fluorescence intensity exhibits a very noticeable decrease for excitation wavelengths shorter than about 300 nm. The relative quantum yield of the fluorescence, as a function of excitation wavelength, can be deduced by dividing the intensity of the fluorescence excitation spectrum at a given wavelength by the intensity of the absorption spectrum at the same wavelength. Although it was not possible to measure the absorption spectrum of the jet-cooled DMABN by cavity ring-down technique over a wide spectral range, comparison of the normalized vapor-phase fluorescence excitation spectrum with the corresponding absorption spectrum, also shown in Figure 1, demonstrates that the fluorescence yield decreases rather dramatically at higher excitation energies. The onset of the strong decrease in the fluorescence yield is about 300 nm, which corresponds to the S_1 (L_b) excess vibrational energy, ΔE, of about 1000 cm^{-1}.

Unlike the fluorescence yield, which is strongly excess-energy dependent under collision-free conditions, the measured lifetime of the emission is almost independent of excitation energy, as shown in Figure 2 and Table 1. The differing behaviors of the

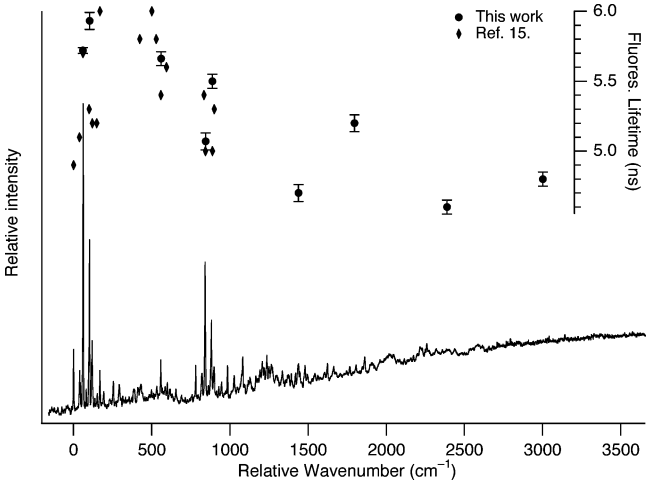

Figure 2. Normalized fluorescence excitation spectrum of DMABN in a free jet. The excess energy is with respect to the origin band at 32 394 cm^{-1}. Inset plots represent the fluorescence lifetimes (in ns), measured as a function of the wavelengths of excitation.

TABLE 1: Fluorescence Lifetimes of DMABN, ABN, and NN as a Function of Excess Vibrational Energy in a Jet Condition

DMABN		ABN		NN	
ΔE (cm^{-1})[a]	τ (ns)	ΔE (cm^{-1})[b]	τ (ns)	ΔE (cm^{-1})[c]	τ (ns)
0	5.72(2)[d]	0	16.54(14)[d]	0	23.9(3)[d]
42	5.93(6)	815	12.44(15)	401	34.0(6)
500	5.66(5)	1630	8.61(14)	450	39.0(8)
785	5.07(6)	1980	7.88(19)	509	33.1(9)
829	5.50(5)			658	35.7(9)
1378	4.70(6)			949	31.1(8)
1736	5.20(6)			1400	31.8(4)
2328	4.60(5)			1945	28.3(4)
2942	4.80(5)			2473	28.0(2)
				3057	24.6(2)

[a] Energies with respect to the DMABN origin band at 308.70 nm (32 394 cm^{-1}). [b] Energies with respect to the ABN origin band at 298.56 nm (33 494 cm^{-1}). [c] Energies with respect to the NN origin band at 318.21 nm (31 425 cm^{-1}). [d] The values in parentheses indicate a standard deviation (1σ).

fluorescence yield (Φ_F) and fluorescence lifetime (τ_F) indicate that the strong decrease in the fluorescence yield at higher excitation energies is due to a large decrease in the S_1 radiative decay rate ($k_r = \Phi_F/\tau_F$), and not due to an increase in S_1 nonradiative decay rate (k_{nr}). The decrease in k_r at higher energies is unrelated to intramolecular vibrational redistribution (IVR), as the radiative transition probability of an allowed electronic transition is expected, and observed,[14] to be unaffected by IVR (and hence S_1 excess vibrational energy). This is because the $S_1 \rightarrow S_0$ radiative decay of the "dark" S_1 vibrational level, produced by IVR, occurs through a sequence transition (involving S_0 vibrational level of same symmetry), which has transition probability essentially identical to that for the "bright" S_1 vibrational level, produced by $S_1 \leftarrow S_0$ excitation.

Figure 3 shows the dispersed fluorescence spectra of DMABN, measured as a function of the excitation wavelength. A striking feature of the dispersed emission is that the sharp, discrete fluorescence from the very low-lying S_1 vibronic levels changes to the broad, structureless fluorescence, characteristic of the states that evolve from IVR[15] at higher excitation energies. The onset of IVR occurs at unusually small (<500 cm^{-1}) S_1 excess vibrational energy, consistent with the presence of several very low-frequency modes associated with the dimethylamine moiety of DMABN.[16] Another striking feature of the dispersed fluorescence is the broadening and the red-shift of its intensity maximum that occurs with increasing excitation energy. The red-shift and the broadening are much more evident when the dispersed fluorescence spectra are displayed in wavenumber scale (not shown). While the loss of sharp feature is a characteristic of an emission from IVR-evolved states, the large broadening and the strong red-shift of the fluorescence with increasing excitation energy cannot be attributed to IVR.[17] Instead, these are the features that are expected when the geometry of the emitting state is significantly different from that of the ground state.[18]

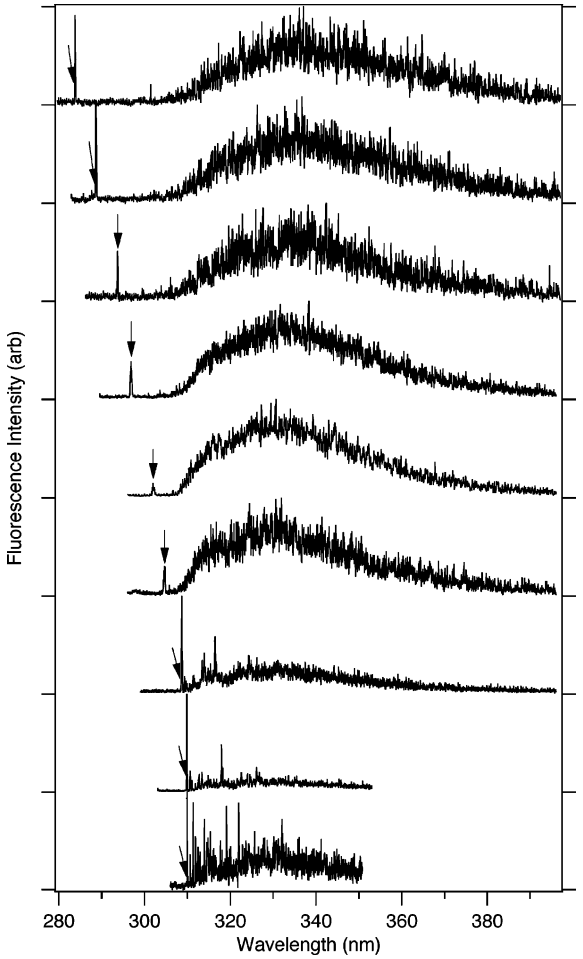

Figure 3. Dispersed fluorescence spectra from various vibronic levels of the electronically excited DMABN in a free jet. The arrows indicate the wavelengths of excitation.

The decrease in the radiative decay rate (k_r) and the change in the spectral shape (broadening and red-shift of the intensity maximum) of the dispersed fluorescence with increasing excitation energy, suggests that the nature of the emitting state changes with S_1 excess vibrational energy. This could occur if a weakly emissive excited-state intersects the higher-lying vibronic levels of the bright state. Such a crossing has indeed been predicted for DMABN by the TDDFT calculation of Zgierski and Lim,[6] which shows that the lowest-energy $\pi\sigma^*_{C\equiv N}$ state of bent geometry (C−C≡N angle of 120°) crosses the lowest-energy $\pi\pi^*$ (L_b) state of linear geometry at CCN angle of about 150°. The barrier for the crossing is about 0.15 eV above the electronic origin of the L_b state, Figure 4. The lowest excited singlet (S_1) state is $\pi\pi^*$ in linear geometry and $\pi\sigma^*$ in the bent geometry. A direct excitation of the $\pi\sigma^*$ state from the ground state is highly inefficient because of the small Franck−Condon factor that arises from the large geometry difference between the two

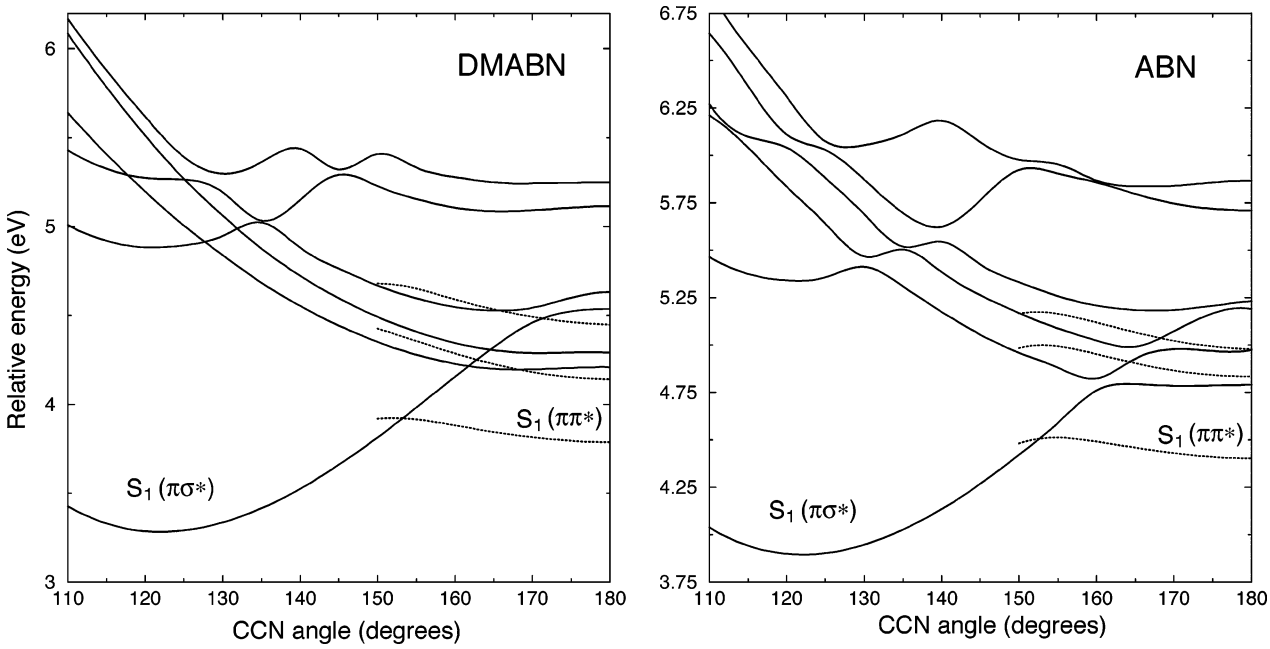

Figure 4. TDDFT energies of low-lying $\pi\pi^*$ and $\pi\sigma^*$ singlet states of DMABN (left) and ABN (right) as a function of C(ring)−C−N angle, as calculated using BP86/6-311++G** level of theory. The solid curves are for the optimized CIS/6-311++G** geometries of $\pi\sigma^*$ state, whereas the dotted curves are for the corresponding optimized $\pi\pi^*$ state (from ref 6 with permission).

states. The weakly emissive $\pi\sigma^*$ state can however be generated by state crossing from the optically excited $\pi\pi^*$ state.

Under the collision-free condition of a supersonic free jet, an irreversible state switch from the $\pi\pi^*$ state to the $\pi\sigma^*$ state is not expected to occur. Nonetheless the emitting state, which is $\pi\pi^*$ below the barrier for $\pi\pi^*/\pi\sigma^*$ crossing, changes into a state that is mostly $\pi\sigma^*$ as the excitation energy exceeds the barrier for the crossing. This state crossing would lead to a dramatic decrease in a radiative decay rate above the barrier, as observed in experiment. Interestingly, the onset of the decrease in k_r occurs at about 1000 cm^{-1} (0.12 eV) above the 0−0 band of the $\pi\pi^*$ (L_b) ← S_0 absorption, consistent with the computed barrier of about 0.15 eV (1200 cm^{-1}). The change in the nature of the emitting state from primarily $\pi\pi^*$ to largely $\pi\sigma^*$ would also lead to the broadening and red-shift of the dispersed fluorescence because of the large geometry difference between the $\pi\sigma^*$ state and the electronic ground state. The lack of a strong excitation-energy dependence of the fluorescence lifetime implies that the nonradiative decay rate of the $\pi\sigma^*$ state is also much smaller than that of the initially excited $\pi\pi^*$ state.

p-Aminobenzonitrile (ABN). Figure 5 displays the normalized fluorescence excitation spectrum of jet-cooled ABN for the wavelength range of 267−300 nm. As in the case of DMABN, the fluorescence intensity of ABN decreases very substantially for excitation wavelengths shorter than about 291 nm. Although the measured fluorescence lifetime of ABN also decreases with decreasing wavelength of excitation, Figure 5 and Table 1, the decrease is much less dramatic than in the case of the fluorescence yield. Thus, as in DMABN, the radiative decay rate of ABN exhibits a significant decrease for S_1 excess vibrational energy exceeding about 870 cm^{-1} (0.11 eV). This threshold energy, which we associate with the barrier for the $\pi\pi^*/\pi\sigma^*$ crossing, is in good agreement with the computed barrier of 0.13 eV (as shown in Figure 4). The smaller threshold energy of ABN relative to that of DMABN, with substantially larger vibrational state density, indicates that the decrease in k_r at higher excitation energies is not due to an IVR-induced change in the radiative property.

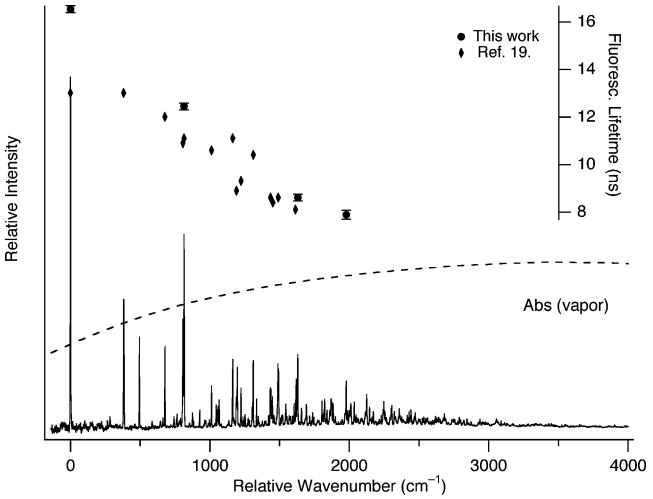

Figure 5. Normalized fluorescence excitation spectrum of ABN in a free jet and vapor-phase absorption spectrum of ABN at about 100 °C (dashed curve). The excess energy is with respect to the origin band at 33 494 cm^{-1}. The inset plots represent the fluorescence lifetimes (in ns), measured as a function of the S_1 excess vibrational energy.

4-Diisopropylaminobenzonitrile (DIABN). The fluorescence excitation spectrum of jet-cooled DIABN has been reported by Daum et al.[9] The spectrum shows evidence for a dramatic decrease in intensity at higher excitation energies. Our normalized excitation spectrum, shown in Figure 6, confirms this earlier work. The energy threshold for the "fluorescence break-off" is around 307 nm ($\Delta E \sim 800$ cm^{-1}), which is somewhat smaller than that for DMABN or ABN. On the basis of our TD/BP86/6-311++G** calculation that places the $\pi\sigma^*_{C\equiv N}$ state below the lowest-energy $\pi\pi^*$ (L_b) state, Figure 7, we would again attribute the fluorescence break-off to the crossing of the $\pi\sigma^*$ state with the optically excited $\pi\pi^*$ state. The dramatic decrease in the relative fluorescence yield at higher excitation energies is evident from a comparison of the fluorescence excitation spectrum with the vapor-phase absorption spectrum, which is also shown in Figure 6.

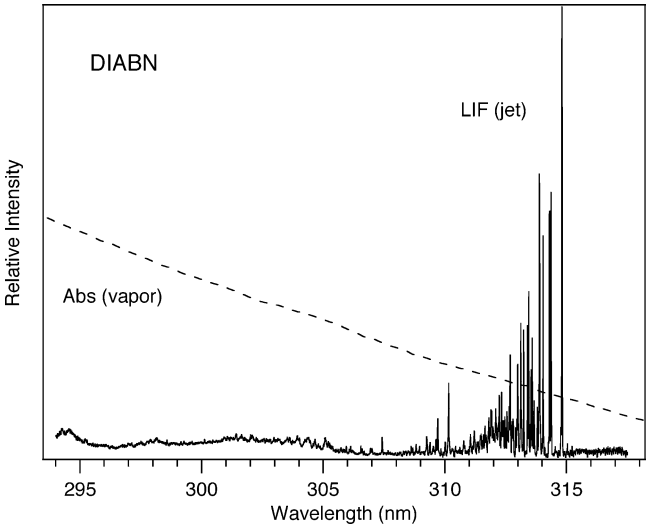

Figure 6. Normalized fluorescence excitation spectrum of DIABN in a free jet (solid curve) and vapor-phase absorption spectrum of DIABN at about 150 °C (dashed curve).

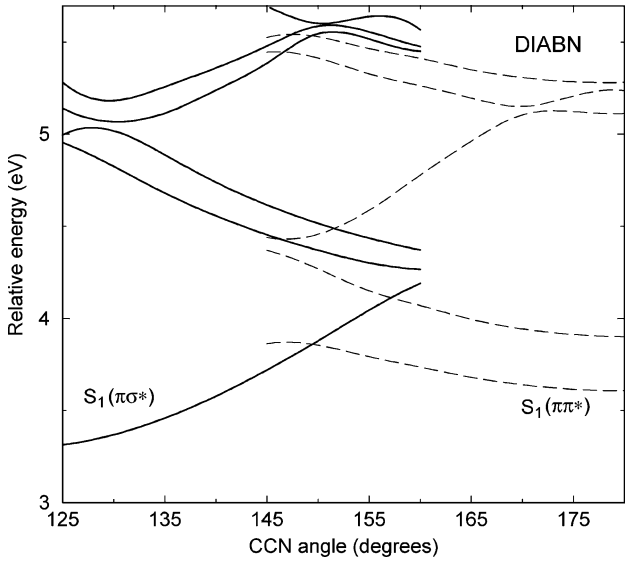

Figure 7. TDDFT energies of low-lying $\pi\pi^*$ singlet states (dashed curve) and $\pi\sigma^*$ singlet states (solid curve) of DIABN at their optimized geometries, as calculated using BP86/6-311++G** level of theory.

1-Naphthonitrile (NN). The photophysical behaviors of NN are very similar to those of DMABN, ABN, and DIABN. Figure 8 presents the fluorescence excitation spectrum of jet-cooled NN and the normalized fluorescence excitation and absorption spectra of the vapor-phase NN. As in the aminobenzonitriles, the fluorescence intensity decreases rather sharply for S_1 excess vibrational energies, exceeding about 1000 cm^{-1} under collision-free conditions. The TD/BP86/6-311++G* energy calculation indicates, however, that the $^1\pi\pi^*/^1\pi\sigma^*$ intersection in NN occurs far away (CCN angle, $\theta \sim 135°$) from the Franck−Condon region ($\theta \approx 180°$) of the $\pi\pi^*$ (L_b) ← S_0 absorption, with a high-energy barrier (~ 0.7 eV) for state crossing, Figure 9. Moreover, the TD energy of the $^1\pi\sigma^*$ state at the optimized CIS/6-311++G** geometry lies at about 0.5 eV above the $\pi\pi^*$ state at its optimized geometry. These results, therefore, indicate that the $^1\pi\pi^*/^1\pi\sigma^*$ state crossing is a highly unlikely source of the fluorescence break-off. A much more likely (and perhaps the most likely) origin of the fluorescence break-off is the crossing between the $\pi\pi^*$ singlet state and the $\pi\sigma^*$ triplet state of lower energy. The CIS/6-311++G** energy calculation

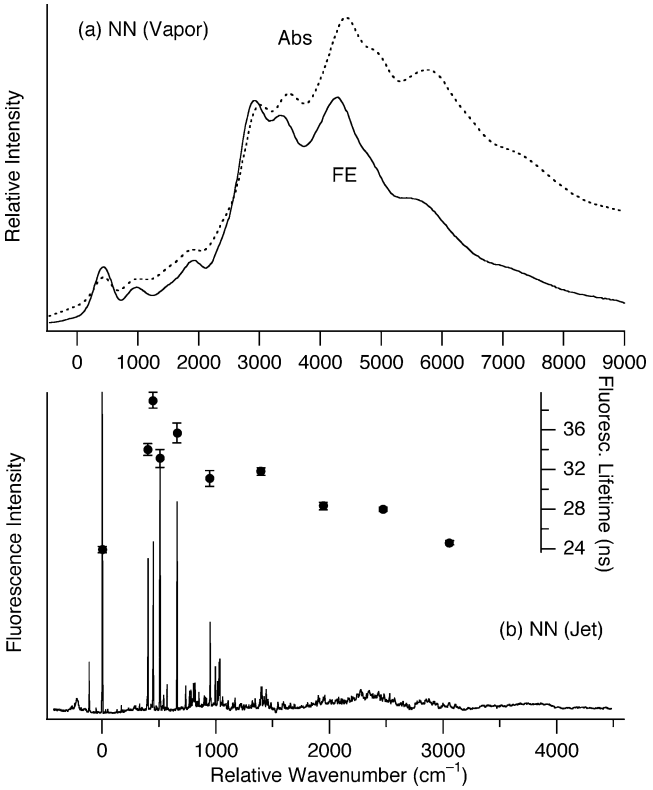

Figure 8. (a) Comparison of fluorescence excitation (solid curve) and absorption spectrum (dashed curve) of a vapor-phase NN at about 50 °C, recorded under a collision-free condition. The excess energy is with respect to the origin band at 31 425 cm^{-1}. The stronger, higher-energy band system commencing at about 0 + 3000 cm^{-1} represents the $\pi\pi^*$ (L_a) ← S_0 absorption. (b) Laser-induced fluorescence excitation spectrum of NN in a free jet. The inset plots represent the fluorescence lifetimes (in ns), measured as a function of the S_1 excess vibrational energy.

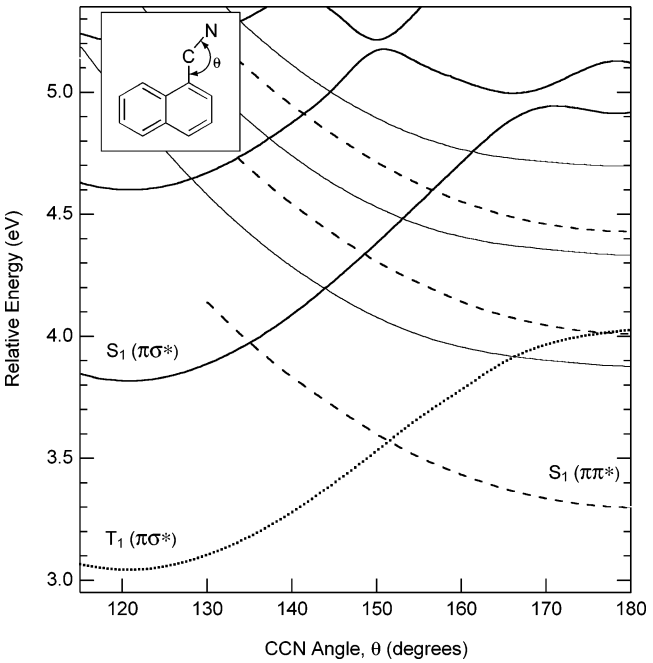

Figure 9. TDDFT energies of low-lying $\pi\pi^*$ singlet states (dashed curve) and $\pi\sigma^*$ singlet states (solid curve) of NN at their optimized geometries, as calculated using BP86/6-311++G** level of theory. The lowest-energy dotted curve represents the $\pi\sigma^*$ triplet state based on the CIS/6-311++G** energy calculation. Inset scheme shows the definition of CCN angle, θ.

shows that the $\pi\pi^*$ singlet state crosses the $\pi\sigma^*$ triplet states, which lies at about 0.26 eV below the minimum of the $\pi\pi^*$ state, at a CCN angle of about 155° with a barrier of about 0.3 eV. We, therefore, attribute the fluorescence break-off in NN to the coupling of the bright $^1\pi\pi^*$ state with the dark $\pi\sigma^*$ triplet state, which leads to a large decrease in the k_r of the excited singlet state at higher energies. The fluorescence lifetime, $1/(k_r + k_{nr})$, of NN is essentially independent of excitation energy, Figure 9 and Table 1, consistent with the very small intrinsic decay rate of the triplet state relative to that of the excited singlet state.

In summary, the results of the present study strongly suggest the existence of a state crossing between the lowest-energy $\pi\pi^*$ and the lowest-energy $\pi\sigma^*$ state. We have proposed that the state coupling involves two excited singlet states ($^1\pi\pi^*$ and $^1\pi\sigma^*$) in aminobenzonitriles (DMABN, ABN, and DIABN), the $\pi\pi^*$ singlet and the $\pi\sigma^*$ triplet states in 1-naphthonitrile (NN). The coupling of the emissive $\pi\pi^*$ state with the "dark" $\pi\sigma^*$ state leads to a large decrease in radiative decay rate, which is responsible for the fluorescence loss. It is our intention to utilize various two-color pump−probe schemes to directly observe the low-lying $\pi\sigma^*$ state in aromatic nitriles and related aromatic alkynes.

Acknowledgment. We are very grateful to the Office of the Basic Energy Sciences of the Department of Energy for support of this work, and to the Ohio Supercomputer Center for grants of computer time.

References and Notes

(1) Zgierski, M. Z.; Lim, E. C. *Chem. Phys. Lett*. **2004**, *387*, 352.

(2) Zgierski, M. Z.; Lim, E. C. *Chem. Phys. Lett*. **2004**, *393*, 143.

(3) Okuyama, K.; Hasegawa, T.; Ito, M.; Mikami, N. *J. Phys. Chem*. **1984**, *88*, 1711.

(4) Hirata, Y.; Okada, T.; Mataga, N. *J. Phys. Chem*. **1992**, *96*, 6559.

(5) Hirata, Y. *Bull. Chem. Soc. Jpn*. **1999**, *72*, 1647.

(6) Zgierski, M. Z.; Lim, E. C. *J. Chem. Phys*. **2004**, *121*, 2462.

(7) Okada, T.; Mataga, N.; Baumann, W. *J. Phys. Chem*. **1987**, *91*, 760.

(8) Kwok, W. M.; Ma, C.; Philis, D.; Matousek, P.; Parker, A. W.; Towrie, M. *J. Phys. Chem. A* **2000**, *104*, 4188.

(9) Daum, R.; Druzhinin, S.; Ernst, D.; Rupp, L.; Schoeder, J.; Zachariasse, K. A. *Chem Phys. Lett*. **2001**, *341*, 272.

(10) Sobolewski, A. L.; Domcke, W. *Chem. Phys. Lett*. **1996**, *250*, 428.

(11) Demeter, A.; Druzhinin, S.; George, M.; Haselbach, E.; Roulin, U. L.; Zachariasse, K. A. *Chem. Phys. Lett*. **2000**, *323*, 351.

(12) Zgierski, M. Z.; Lim, E. C., unpublished results.

(13) Platt, J. R. *Systematics of the Electronic Spectra of Conjugated Molecules*; Wiley: New York, 1964.

(14) Huang, C.-S.; Hsiek, J. C.; Lim, E. C. *Chem. Phys. Lett*. **1974**, *28*, 130.

(15) Parmenter, C. S. *Faraday Discuss. Chem. Soc*. **1983**, *75*, 7.

(16) Saigusa, H.; Miyakoshi, N.; Mukai, C.; Fukagawa, T.; Kohtani, S.; Gordon, R. *J. Chem. Phys*. **2003**, *119*, 5414, and references therein.

(17) Lim, E. C. In *Advances in Photochemistry*; Necker, D. C., Volman, D. H., van Bünau, G., Eds.; John Wiley: New York, 1997; Vol. 23, p 165.

(18) Zgierski, M. Z.; Fujiwara, T.; Lim, E. C. *J. Chem. Phys*. **2005**, *122*, 144312.